

Simulation of unsteady flows by the DSMC Macroscopic Chemistry Method

Mark Goldsworthy Michael Macrossan Madhat Abdel-jawad

*Centre for Hypersonics, School of Engineering, University of Queensland,
Brisbane, Australia 4072*

Abstract

In the Direct Simulation Monte Carlo (DSMC) method, a combination of statistical and deterministic procedures applied to a finite number of ‘simulator’ particles are used to model rarefied gas-kinetic processes. In the Macroscopic Chemistry Method (MCM) for DSMC, chemical reactions are decoupled from the specific particle pairs selected for collisions. Information from all of the particles within a cell, not just those selected for collisions, is used to determine a reaction rate coefficient for that cell. Unlike particle-based methods, MCM can be used with any viscosity or non-reacting collision models and any non-reacting energy exchange models. It can be used to implement any reaction rate formulations, whether these be from experimental or theoretical studies. MCM has been previously validated for steady flow DSMC simulations. Here we show how MCM can be used to model chemical kinetics in DSMC simulations of unsteady flow. Results are compared with a collision-based chemistry procedure for two binary reactions in a 1-D unsteady shock-expansion tube simulation. Close agreement is demonstrated between the two methods for instantaneous, ensemble-averaged profiles of temperature, density and species mole fractions, as well as for the accumulated number of net reactions per cell.

1 Introduction

The standard method for including chemical reactions in rarefied Direct Simulation Monte-Carlo (DSMC) solvers, the total collision energy (TCE) method [1] suffers from a number of limitations. Firstly, it can only deal with reaction rates in the Arrhenius form and thus cannot always represent chemical reaction rate data derived from theory or experiments. Secondly, TCE can only be used with one particular collision model, the variable hard sphere model, and is thus limited to modelling a gas with a ‘power-law’ viscosity $\mu = \mu_r (T/T_r)^\omega$. In contrast, a typical continuum CFD solver may use reaction rate data in a variety of functional forms, and may use a more realistic variation of viscosity with temperature. This could be important for the development of hybrid continuum/DSMC solvers since the gas properties in the continuum solver are restricted to the limited range allowed by the DSMC solver.

The limitations of TCE arise from the fact that it is a collision-based procedure in which chemical reactions can only occur when simulator particles of the right kind are selected to undergo a collision. Although this seems to be well founded on physical grounds, the collision selection procedures are dictated by the DSMC collision model which is itself an approximation; the distribution of collision energies is governed by the required average rate of momentum transfer (*i.e.* the simulation gas viscosity). This distribution of collision energies may be plausible, but there is no guarantee that it is accurate enough to reproduce experimentally observed reaction rates when combined with a simple steric factor (probability of reaction for a given collision pair).

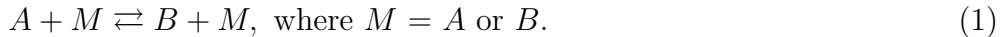
To overcome these difficulties the Macroscopic Chemistry Method (MCM) was proposed by Lilley and Macrossan [2] and refined by Goldsworthy *et al.* [3,4]. In this method, the rates of chemical reactions are largely decoupled from the collision procedures; any collision models such as the Lennard-Jones or Morse potentials can be used. In MCM, chemical reactions are computed by solving the chemical kinetic equations at the end of each time-step using macroscopic information obtained from *all* the simulator particles in a cell, not just those selected for collisions. The macroscopic method has been used with a variety of temperature and multi-temperature dependent reaction rates [2,5], and with reaction rates which depend on the local density as well as temperature [2].

We have previously shown [3] that, because MCM assumes only that the steric factor is the same for equilibrium and non-equilibrium conditions, it produces plausible non-equilibrium reaction rates. On the other hand, when TCE is applied in highly non-equilibrium conditions, the reaction rates arise from a variation in the steric factor which has no basis in theory or experiment but is dictated purely for reasons of mathematical tractability. Although this is not known to be a serious problem with TCE, it is one that does not arise for

MCM.

The Macroscopic Chemistry Method has been extensively tested for steady flows [3–6], though it has not been applied to unsteady flows. Important insight may be gained into the fluid dynamics of a particular problem by observing the transient fluid motion. In some cases, the flow-field is inherently unsteady and transient simulations are necessary. Here we propose a procedure for implementing MCM for unsteady flows. We test this procedure by calculating the unsteady flow in a shock tube, for a ‘model’ reacting gas. We do not present this ‘model gas’ as an improved collision-based chemistry procedure for DSMC, or to suggest that the reaction rates arising from this model are superior to those arising from other collision-based chemistry procedures. We use the model to show that the macroscopic method can (a) reproduce approximate reaction rates for any collision-based procedure for which the equilibrium reaction rates can be determined theoretically, and (b) can do so for unsteady flows.

The model gas has two species. Species A may be converted to species B , or B into A , through the reactions



Here M is the collision partner. The $A \rightarrow B$ reaction is endothermic, with heat of reaction $-E_a$ ($\equiv -k\theta_a$). Except for their chemical potential energy, species A and B molecules are assumed to be identical in all other respects. Note that we have chosen not to compare MCM directly with TCE because here we are interested in testing the unsteady implementation of MCM exclusively. We compare the MCM results with those from a particle-based chemistry procedure appropriate to this model gas and guaranteed to return *exactly* the same reaction rates as MCM in steady flows.

2 Procedure for unsteady flows

The DSMC method is appropriate for a dilute gas assumption in which three body collisions may be ignored. For a general reaction $A + B \rightarrow \text{products}$, the rate of reactant depletion can be expressed as

$$\Delta \dot{N}_A = k_f N_A N_B / V. \quad (2)$$

Here N_A is the number of species A particles in a region of volume V and k_f (m^3/s) is the reaction rate coefficient for the forward reaction. In MCM, the required change, $\Delta N_A = \Delta \dot{N}_A \Delta t$, in the number of a given species A

over a computational time-step Δt is calculated using an expression for $\Delta \dot{N}_A$ similar to Eq. 2. Then the numbers of each species are adjusted to account for this required ΔN_A . For steady flows, N_A and N_B in Eq. 2 are replaced by their time-averaged values, \bar{N}_A and \bar{N}_B and this leads to the correct reaction rate in the limit of a large sample. For unsteady flows, time averaged values cannot be employed and direct use of Eq. 2 would lead to incorrect ensemble averaged reaction rates since $\overline{N_A N_B} \neq \bar{N}_A \bar{N}_B$.

A similar problem arises when setting the simulator collision rate in unsteady flows. The number of collisions per unit time amongst N particles is proportional to NN/V . For steady flows, using the NTC method, Bird [7] set the collision rate as proportional to $N\bar{N}/V$, where N is the instantaneous number of simulator particles in a cell, and \bar{N}/V is the latest (time-averaged) estimate of the simulator number density. In contrast, Bird [8] has proposed that $N(N-1)/V$ be used in place of $N\bar{N}/V$. He shows that if the fluctuations in N are distributed according to a Poisson distribution, then $\overline{N(N-1)} = \bar{N}\bar{N}$ and the correct collision rate is obtained. In unsteady simulations, for which the time-averaged number density \bar{N}/V is not available, we use the new procedure to set the collision rate and we model instantaneous chemical rates in a similar way.

The net change in the number of simulator particles of species A , over a time-step Δt , due to the reaction $A + M \leftrightarrow B + M$ where $M = A, B$ is computed using

$$\begin{aligned} \Delta N_A = & \frac{1}{2} [k_{b_{M=B}} N_B (N_B - 1) - k_{f_{M=A}} N_A (N_A - 1) + \\ & + 2(k_{b_{M=A}} - k_{f_{M=B}}) N_A N_B] \frac{W \Delta t}{V}. \end{aligned} \quad (3)$$

In this expression the term $N_A(N_A - 1)$ is evaluated only for $N_A \geq 1$ and similarly the term $N_B(N_B - 1)$ is evaluated only for $N_B \geq 1$. W is the number of real particles represented by each DSMC simulator particle. Since Δt is necessarily smaller than the mean collision time, ΔN_A is usually a fractional number. Thus, the value of ΔN_A is compared to a random fraction; a reaction is processed if the random number is larger than ΔN_A . In the case where $\Delta N_A > 1$, $[\Delta N_A]$ reactions are processed and the remainder is compared to a random fraction. This procedure ensures that there is no delay in processing reactions and that the correct number of reactions are modelled in the limit of a large ensemble average.

When the reaction rate coefficient k_f is given as a function of temperature, MCM uses the total energy of the simulator particles in the cell to estimate the temperature required to evaluate k_f . Here we use the variance of the sample population to evaluate the kinetic temperature; the statistical implications of

this are discussed in §5.

For a multi-species gas, the mean translational energy of species s is given by

$$\langle E_s \rangle = \frac{m_s}{2N_s^2} \sum_{i=x,y,z} \left[N_s \sum v_i^2 - \left(\sum v_i \right)^2 \right]. \quad (4)$$

Here m_s is the mass of one particle and N_s is the number of simulator particles representing species s in the cell. The overall translational temperature follows as

$$T = \frac{2}{3k} \left[\frac{1}{N} \sum_s N_s \langle E_s \rangle \right], \quad (5)$$

where k is Boltzmann's constant. When a reaction must be implemented in the macroscopic method, reactant particles (in this case, selected at random from the cell) are converted into product species particles, ensuring that the total mass, momentum and kinetic energy of the products is the same as that for the reactants. The total net change in chemical energy due to all reactions in a cell is removed from the thermal energy of all particles in the cell; thus the mean particle velocity must be calculated in each cell at each time step. The details of these procedures are given by Lilley and Macrossan [2]. The calculation of the cell mean velocity and cell kinetic temperature, requires little computational expense. The procedure may be added to a DSMC code by implementing a separate chemistry step after the calculation of collisions

$$move \rightarrow index \rightarrow collide \rightarrow chemistry.$$

Since DSMC and MCM, with the modified collision rate procedure, uses only information from the particles in a given cell at the current time-step, the methods are readily applied to multiple independent simulations on parallel processor systems.

3 Chemical rate equations for the model gas

Except for their chemical potential energy, the A and B species of the model gas have the same properties as argon; they have no rotational or vibrational energy storage modes. The variable hard sphere [1] (VHS) collision model is employed with the modified NTC collision procedure, *i.e.* with $N(N-1)/V$ in place of $N\bar{N}/V$. The collision cross-section is such that the Chapman-Enskog viscosity is given by $\mu = \mu_r (T/T_r)^\omega$, where $\mu_r = 2.3 \times 10^{-5}$ (kg/m/s), $T_r = 300$ K and $\omega = 0.72$. The only reactions are those in Eq. 1. The reaction

rates are taken to be those produced by the following particle-based chemistry model.

In the particle chemistry model, $S_f = 0.2$ and $S_b = 0.001$. Let E_c be the centre of mass energy of the collision pair then:

- (1) $A - A$ pairs with $E_c > E_a$ become $B - A$ with probability S_f
- (2) $B - B$ pairs become $A - B$ with probability S_b
- (3) $A - B$ pairs with $E_c > E_a$ become
 - (a) $B - B$ with probability S_f
 - (b) $A - A$ with probability S_b
- (4) $A - B$ pairs with $E_c < E_a$ become $A - A$ with probability S_b .

In order to match the particle-based results with MCM, we require the theoretical reaction rate coefficient produced by the particle method. The corresponding forward and backward reaction rate coefficients may be expressed as

$$k_f = Z_c F S_f \text{ and } k_b = Z_c S_b. \quad (6)$$

Here F is the fraction of VHS collision pairs with collision energy greater than E_a and Z_c (m^3/s) is the VHS collision constant. Under thermal equilibrium conditions Z_c is given by

$$Z_c = \frac{1}{f_s} \frac{15kT_r}{2\mu_r (2.5 - \omega) (3.5 - \omega)} \left(\frac{T_r}{T} \right)^{\omega-1}, \quad (7)$$

where $f_s = 2$ for $A - A$ and $B - B$ collisions and $f_s = 1$ for $A - B$ collisions, and F is given by

$$F = \Gamma(2.5 - \omega, E_a/kT). \quad (8)$$

Note that these rate coefficients are not in the simple Arrhenius form.

In MCM, the thermal equilibrium reaction rates evaluated from the given rate coefficients, in this case those in (6) - (8), are multiplied by two ‘rate correction factors’ ψ_Z and ψ_F as described by Goldsworthy *et al.* [3]; this accounts for the deviation between the non-equilibrium collision rate for colliding particle pairs with $E_c > E_a$ found in the MCM collision procedure and the corresponding thermal equilibrium value derived from the cell temperature. Note that we could have implemented an analytic model for the nonequilibrium reaction rate such as that given by Baras and Mansour [9]. Instead, the method employed here uses the actual nonequilibrium distribution as obtained from the DSMC simulation.

4 Shock-expansion tube simulation

We have applied the transient MCM procedures to simulations of an unsteady 1-D flow in a shock-expansion tube, filled with the model gas described in §3. The initial condition consists of two regions, both at rest and with temperatures $T_{\text{left}} = 1000$ K and $T_{\text{right}} = 100$ K. The chemical activation temperature was $\theta_a = 5000$ K. The density ρ is uniform along the tube and all cells are contain equal numbers of both species.

Results are normalized by a nominal mean free path $\lambda_{\text{left}} = 2\mu/\rho\bar{c}$ where $\bar{c} = \sqrt{8kT/m\pi}$ is a characteristic thermal speed and μ is the gas viscosity, both evaluated for $T = T_{\text{left}}$. The characteristic time is $\tau_{\text{left}} = \lambda_{\text{left}}/\bar{c}$. Since the forward reaction rate coefficient k_f is independent of density, the normalized results apply to any density ρ .

Instantaneous results are output at $t = 500\tau_{\text{left}}$. A total of 2000 computational cells ($\Delta x = 0.066\lambda_{\text{left}}$) span the domain. Simulations using the particle and macroscopic chemistry methods with 5×10^4 particles were run. For each case, results from 1000 separate simulations were combined. Profiles of density, temperature and mole fraction of species A are shown in Figures 1, 2 and 3 respectively.

MCM results are shown as solid lines; particle chemistry results are plotted every 25th cell using circles. No spatial or time averaging is used. A shock wave has propagated from the high temperature (high pressure) region toward the low temperature (low pressure) region a distance of approximately $28.5\lambda_{\text{left}}$. The shock wave spans almost $3.5\lambda_{\text{left}}$. An expansion wave can be seen moving through the high temperature region. Neither the shock nor the expansion wave has been reflected from the end walls at this elapsed time. Since both forward reactions are exothermic and have an activation temperature $E_a/k = 5 \times T_{\text{left}}$, the forward reactions resulting in $A \rightarrow B$ transitions are much faster in the higher temperature region and act to lower the temperature there. The reverse transitions $B \rightarrow A$ are endothermic and the rate at which they occur is proportional to the collision rate. The temperature in the undisturbed region in front of the shock is slightly higher than the initial value because of these endothermic reactions. The mole fraction of species A reaches a maximum value behind the propagating shock wave where the high density and hence collision rate and relatively low temperature favour the $B \rightarrow A$ reaction. It is apparent from these plots that a very close agreement is obtained between the MCM and particle-based chemistry methods.

The accumulated number of net reactions (forward reactions minus reverse reactions) per cell is shown in Figure 4 where close agreement can be seen between the particle and macroscopic chemistry methods. Unlike the previ-

ous figures, which showed ensemble averaged instantaneous results, Figure 4 shows the *accumulated* number of reactions in each cell over the entire simulation time. It can be seen that the forward reaction dominates in the high temperature regions (on the left) and the reverse reaction dominates in the low temperature regions (on the right).

5 Discussion

MCM has been previously shown [2] to be more efficient than the TCE particle chemistry method in a 2-D blunt body flow, in part because only net reactions are computed. The efficiency is highly dependent on the details of the problem. For instance, MCM is more efficient as the number of reactions increases. For the simulations considered here MCM required 50% more CPU time than the particle-based method. However, this value does not indicate the true computational cost of the new method for a number of reasons:

- (1) We evaluated the reaction rate using equations (6) - (8) at each DSMC time-step whereas in most practical applications, the reaction rate would be implemented directly in a simpler mathematical form such as an Arrhenius rate. In that case separate evaluation of Z and F which involves computation of the incomplete gamma function, would not be necessary.
- (2) We modelled only two reactions. Since the computational cost of redistributing the chemical potential energy amongst the particles in a cell is independent of the actual number of reactions occurring, the comparative cost of MCM would be less for simulations involving many reactions.
- (3) We considered only 1-D simulations at a relatively low density, for which the computational cost is almost entirely due to the movement and collision (chemistry) routines. In higher dimensional simulations, the CPU time required to locate and index particles increases and in higher density flows the CPU required to calculate non-reacting collision events increases.

For all these reasons, the CPU time devoted to the MCM chemistry procedures is proportionally less in practical applications.

Because we have matched MCM to the reaction rates produced by a particle method it should not be assumed that we consider the particle method to be more accurate, or better able to match actual reaction rates produced by real molecules. There are many unknowns involved in modelling reacting collisions in DSMC. In this state of ignorance we suggest the safest thing to do is to use only that information which we do know, the equilibrium reaction rates derived from experiment or theory, which MCM uses directly. MCM makes one other assumption to determine the reaction rates when the molecular

energy distribution departs from the equilibrium distribution for which the reaction rates are known; as discussed by Goldsworthy *et al.* [3], the reaction rate is modified by the non-equilibrium fraction of collision pairs in the high energy portion of the distribution. MCM assumes only that the steric factor, the probability that sufficiently energetic collisions will result in a reaction, is the same in a non-equilibrium state as in the nearby equilibrium condition.

One further point should be mentioned. Even if real molecules behaved exactly as those of our model gas, it is possible that, because of the finite sample size in DSMC, the reaction rate per particle might be different in the simulation from that in the real gas. In MCM we could possibly account for this effect when we calculate the cell temperature by using the best estimate of the unknown ‘parent population’ variance, *i.e.* $\sum_{i=1}^N (x_i - \bar{x})^2 / (N - 1)$, rather than the finite sample variance which we did use. This measure of cell temperature did produce slightly different results (not shown here). However the correct method is that which yields, in the limit of a large ensemble-averaged sample, results which are independent of the average number of particles per cell. Use of Eqs. 4 and 5 lead to identical (to within the scatter shown in the figures) results for large accumulated samples regardless of the instantaneous number of simulator particles per cell used in each run. Use of the ‘parent population’ variance lead to a dependence of the results on the number of simulator particles per cell. Hence, we have used the instantaneous temperature when computing the reaction rates. All final (output) results were obtained by combining those from multiple independent DSMC simulations using the appropriate summation techniques as discussed by Garcia [10].

6 Conclusion

We have shown how the macroscopic chemistry method may be used to obtain results in agreement with a particle-based chemistry method in an *unsteady* shock-expansion simulation. In traditional DSMC, macroscopic information in the form of the number density is used to determine the simulator collision rate. The same information is needed in MCM to set the reaction rates, and we have followed Bird in replacing the time averaged simulator number density in a cell \bar{N}/V by $(N - 1)/V$ in setting both the collision rate and the reaction rate in unsteady simulations where \bar{N} is unavailable.

In the macroscopic chemistry method we also use information from the kinetic energy of all the particles in the cell (*i.e.* the kinetic temperature); similar information is obtained in the particle-based method by sampling of particle pairs for possible collisions. In addition, the reaction rate in the particle-based method depends on the non-equilibrium distribution of particle energies in collision pairs; in MCM the analogous non-equilibrium information is extracted

by comparing the actual simulator particle collision rate for high energy pairs with the expected equilibrium value, and adjusting the reaction rate accordingly.

The primary advantage of the macroscopic approach is that any general reaction rate data may be used with any DSMC collision model, without the need for calibration; thus different reaction rate mechanisms involving large numbers of reactions can be quickly implemented and compared.

References

- [1] Bird, G.A, ‘Simulation of multi-dimensional and chemically reacting flows’, *Rarefied Gas Dynamics: Proceedings of the 11th International Symposium*, edited by R. Campargue, Vol. 1, Paris, 1979, pp. 365–388.
- [2] Lilley, C. R. & Macrossan, M. N., ‘A macroscopic chemistry method for the direct simulation of gas flows’, *Physics of Fluids A*, Vol. **16**, No. 6, 2004, pp. 2054-2066
- [3] Goldsworthy, M., Macrossan, M. N. & Abdel-jawad. M., ‘Non-equilibrium reaction rates in the macroscopic chemistry method for DSMC calculations’, *Physics of Fluids*, Vol. **19**, No. 5, 2007, 066101
- [4] Goldsworthy, M., Macrossan, M. N. & Abdel-jawad. M., ‘Multiple reactions and trace species in the DSMC macroscopic chemistry method’, *Physics of Fluids*, Vol. **19**, No. 11, 2007, 116102
- [5] Lilley, C. R. and Macrossan, M. N. ‘Modeling vibrational-dissociation coupling with the macroscopic chemistry method’, *Rarefied Gas Dynamics: Proceedings of the 24th International Symposium*, edited by M. Capitelli, *AIP Conference Proceedings*, Vol. 762, (American Institute of Physics), 2005, pp. 1019–1024
- [6] Lilley, C. R. and Macrossan, M. N. ‘Applying the Macroscopic Chemistry Method to Dissociating Oxygen’, *Rarefied Gas Dynamics: Proceedings of the 25th International Symposium*, edited by M. S. Ivanov and A. K. Rebrov, (Siberian Branch of the Russian Academy of Sciences), 2007, pp. 367–372
- [7] Bird, G. A. *Molecular Gas Dynamics and the Direct Simulation of Gas Flows*, Clarendon Press (Oxford), 1994.
- [8] Bird, G.A, ‘Sophisticated DSMC’, Notes from DSMC07 meeting, Santa Fe, September 2007, available at:
<http://www.gab.com.au/Resources/DSMC07notes.pdf>. (Accessed 7 Nov 2007).
- [9] Baras, F. and Mansour, M., ‘Validity of macroscopic rate equations in exothermic chemical systems’, *Physics Review Letters*, Vol. **63**, No. 21, 1989, pp. 2429-2432.
- [10] Garcia, A., ‘Estimating hydrodynamic quantities in the presence of microscopic fluctuations’, *Communications in Applied Mathematics and Computational Science*, Vol. **1**, 2006, pp. 53-78.

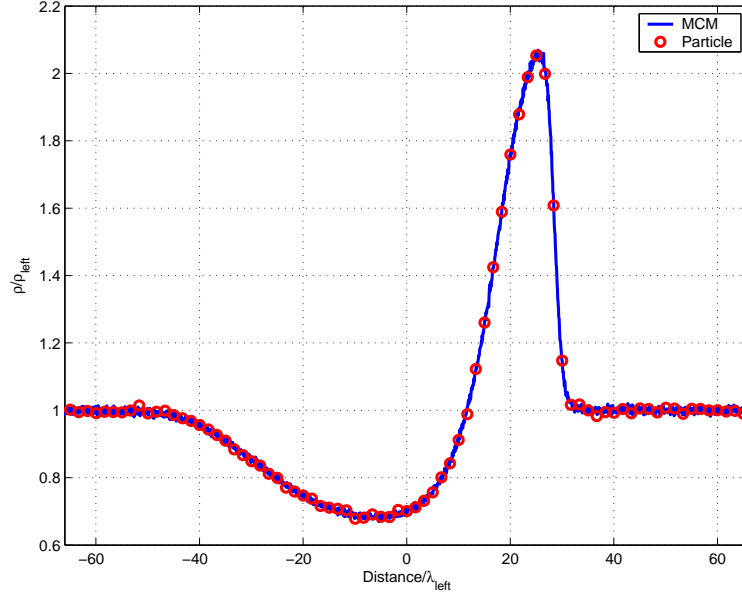


Fig. 1. Ensemble averaged density profiles at simulation time $t = 500\tau_{\text{left}}$ for macroscopic and particle-based chemistry simulations. Particle results are shown for every 25th cell only.

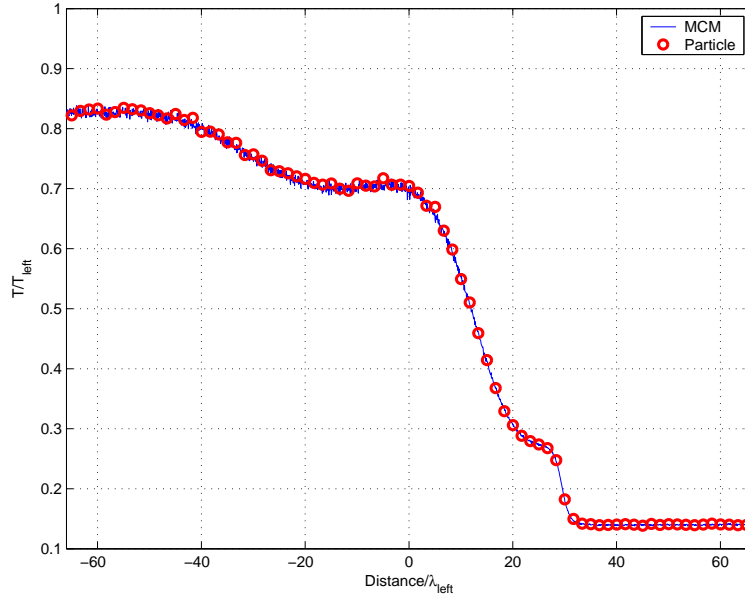


Fig. 2. Ensemble averaged temperature profiles normalized by the initial temperature in the left region at simulation time $t = 500\tau_{\text{left}}$ for macroscopic and particle-based chemistry simulations. The initial temperature ratio separating the left and right regions is 10. Particle results are shown for every 25th cell only.

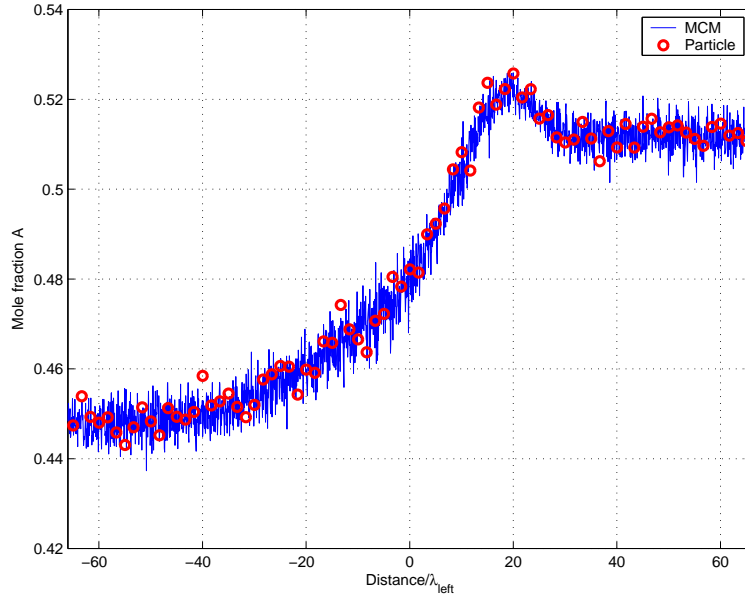


Fig. 3. Ensemble averaged profiles of species A mole fraction at $t = 500\tau_{\text{left}}$. The initial condition consists of $X_A = 0.5$ throughout the entire domain. The rate of exothermic $A \rightarrow B$ reactions increases rapidly with increasing temperature. The rate of the reverse endothermic reaction is proportional to the collision rate. Particle results are shown for every 25th cell only.

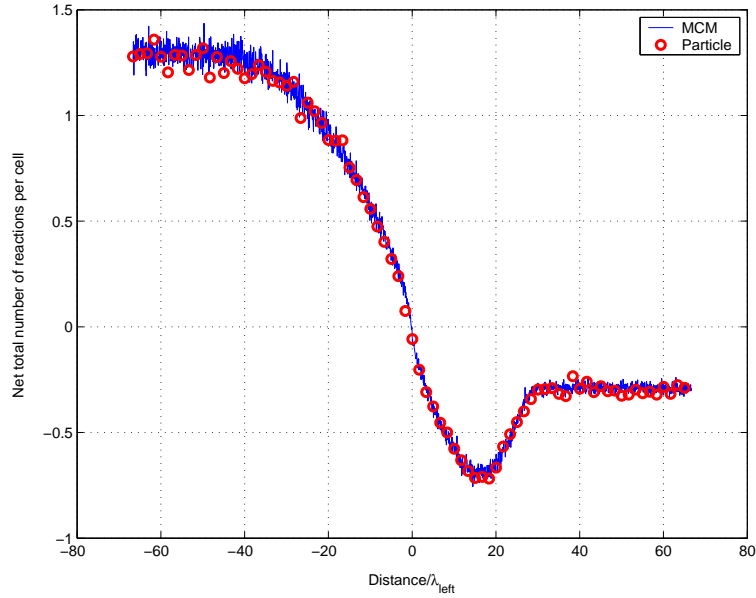


Fig. 4. Accumulated number of net (forward minus reverse) reactions per cell during the unsteady simulation up to $t = 500\tau_{\text{left}}$. Particle results are shown for every 25th cell only.